

Development of Novel Decarboxylation-Urea Method toward Interlayer-Anion-Controlled Layered Double Hydroxides

Masahiro Uga, Yusuke Taniguchi, Mitsuhiro Matsumoto, Takuya Okada, Kazuki Maeda, Eiko Mieda, Katsumi Katakura, and Hirohisa Yamada*



Cite This: *ACS Omega* 2023, 8, 36199–36206



Read Online

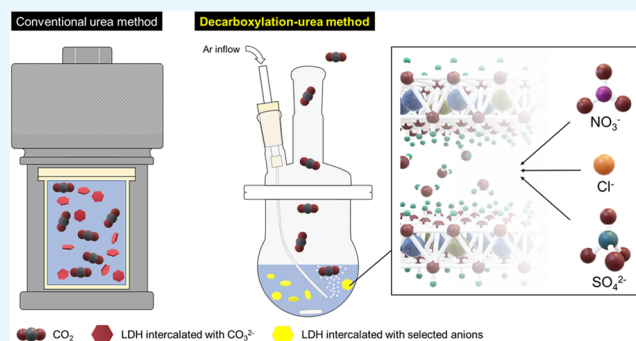
ACCESS |

Metrics & More

Article Recommendations

Supporting Information

ABSTRACT: Layered double hydroxides (LDHs) are representative of a 2D anionic clay. Simple and homogeneous synthesis of interlayer-anion-controlled LDH is essential for studies and industrial production. In this study, we report the one-pot synthesis of an LDH that is selective for interlayer anions, which was labeled as “decarboxylation-urea method”. We obtained LDHs intercalated with NO_3^- , Cl^- , and SO_4^{2-} by removing CO_2 in this method. The ionic conductivities of the prepared LDHs were investigated for their applicability to electrolytes, and it was found that Zn–Al LDH intercalated with NO_3^- showed the highest ionic conductivity (18 mS cm^{-1}). Therefore, the LDH intercalated with NO_3^- synthesized using the decarboxylation-urea method is promising as an alkaline solid electrolyte.



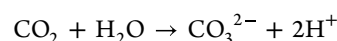
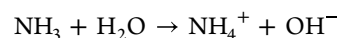
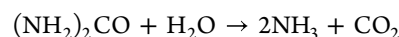
INTRODUCTION

Layered double hydroxide (LDH) is a hydrotalcite-like compound and expressed by the following formula: $[\text{M}_{1-x}^{2+}\text{M}_x^{3+}(\text{OH})_2][\text{A}^{n-}_{n-x}\cdot\gamma\text{H}_2\text{O}]$, where M^{2+} is a divalent metal cation (Mg^{2+} , Co^{2+} , or Ni^{2+}), M^{3+} is a trivalent metal cation (Al^{3+} , Ga^{3+} , or Fe^{3+}), and A^{n-} is an interlayer anion (CO_3^{2-} , NO_3^- , or Cl^-). Similar to the brucite structure of $\text{Mg}(\text{OH})_2$, LDH is characterized by a metal hydroxide layer that is positively charged when a fraction of divalent metal cations is substituted by trivalent metal cations. Anions are intercalated between hydroxide layers together with water molecules to maintain electroneutrality.^{1–5}

LDHs have several characteristics, such as being environmentally friendly, having high biocompatibility, intercalation of organic anions, and proton or hydroxide ion conduction. Hence, LDHs have been widely studied for applications such as water treatment, CO_2 adsorbents, drug delivery systems, and ion-exchange hosts, for which LDHs should selectively intercalate and deintercalate desired anions.^{6–12} Since the ionic conductivity of LDH depends on the interlayer anion species, such a technique is also essential for applications in charge transport carriers such as electrode components.^{13–19} Despite that, it is still difficult to intercalate the desired anion into LDH because CO_3^{2-} -intercalated LDHs are preferentially obtained. In addition, it is also not easy to exchange CO_3^{2-} with other anion species under ambient conditions.^{2,20,21}

For LDH synthesis, coprecipitation is a commonly used procedure. The LDH is precipitated by adding an alkaline solution to a mixture of divalent and trivalent metal salts

dissolved in water to adjust the pH of the solution.^{4,22–24} This method intercalates anions into LDH by dissolving them in solution. However, the size, shape, and homogeneity of the crystals are difficult to control because an increase in local pH leads to inhomogeneous crystallization. The urea method, also known as homogeneous precipitation, is another well-known method. In this method, urea dissolved in a metal salt solution is hydrolyzed by heating the solution as follows



The pH increases slightly, followed by the homogeneous crystallization of LDH. However, a significant amount of time is required to obtain homogeneous hexagonal particles of the desired sizes because the crystals grow slowly. Additionally, only CO_3^{2-} , which stems from the hydrolysis of urea, is intercalated into the LDH.^{25–29} These methods are often combined with hydrothermal processes, wherein the metal salt solution is heated in a Teflon-lined autoclave over $100 \text{ }^\circ\text{C}$ to

Received: June 29, 2023

Accepted: September 6, 2023

Published: September 20, 2023



Table 1. Preparation Conditions and Interlayer Anions of Layered Double Hydroxides (LDHs)

sample ^a	method	interlayer anion	feed molar ratio			divalent metal salt	atmosphere
			Zn ²⁺	Al ³⁺	urea		
H-CO ₃ ²⁻ (2:1:9)	urea + hydrothermal	CO ₃ ²⁻	2	1	9	Zn(NO ₃) ₂ ·6H ₂ O	
U-CO ₃ ²⁻ (2:1:9)	urea	CO ₃ ²⁻	2	1	9	Zn(NO ₃) ₂ ·6H ₂ O	Air
U-NO ₃ ⁻ (2:1:3)	urea	NO ₃ ⁻	2	1	3	Zn(NO ₃) ₂ ·6H ₂ O	Air
D-NO ₃ ⁻ (2:1:9)	decarboxylation-urea	NO ₃ ⁻	2	1	9	Zn(NO ₃) ₂ ·6H ₂ O	Ar
D-NO ₃ ⁻ (3:1:9)	decarboxylation-urea	NO ₃ ⁻	3	1	9	Zn(NO ₃) ₂ ·6H ₂ O	Ar
D-NO ₃ ⁻ (4:1:9)	decarboxylation-urea	NO ₃ ⁻	4	1	9	Zn(NO ₃) ₂ ·6H ₂ O	Ar
D-NO ₃ ⁻ (2:1:3)	decarboxylation-urea	NO ₃ ⁻	2	1	3	Zn(NO ₃) ₂ ·6H ₂ O	Ar
D-NO ₃ ⁻ (2:1:6)	decarboxylation-urea	NO ₃ ⁻	2	1	6	Zn(NO ₃) ₂ ·6H ₂ O	Ar
D-Cl ⁻ (2:1:9)	decarboxylation-urea	Cl ⁻	2	1	9	ZnCl ₂	Ar
D-SO ₄ ²⁻ (2:1:9)	decarboxylation-urea	SO ₄ ²⁻	2	1	9	ZnSO ₄ ·7H ₂ O	Ar

^aThe samples were named on the basis of the synthesized method, interlayer anion, and feed molar ratio of the divalent metal salts. For example, the Zn–Al LDH in the 1st row was synthesized by the urea method combined with the hydrothermal process together with CO₃²⁻-based metal salts (ZnCO₃ and Al₂(CO₃)₃), where the feed molar ration of ZnCO₃, Al₂(CO₃)₃, and urea were 2:1:9. Therefore, we named this sample “H–CO32-(2:1:9)”. Here, (i) the urea method combined with the hydrothermal process, (ii) urea method, and (iii) decarboxylation-urea method were abbreviated as “H”, “U”, and “D”, respectively.

improve crystallinity. However, the combined methods require additional steps to afford a favorable LDH even in the coprecipitation method. Therefore, the interlayer anions of the LDH synthesized via urea hydrolysis are often exchanged using an ion-exchange and reconstruction method. In the ion-exchange method, the interlayer anions of the prepared LDH are exchanged with thermodynamically more stable anions by soaking them in a solution of selected anions.² While in the reconstruction method, LDH is calcined before the soaking process to form a metal oxide, which can reproduce LDH by rehydration. The anions in the solution are then intercalated simultaneously. However, the morphology of the reproduced LDH is transformed.^{21,30,31} Methods such as sol–gel, manual grinding, ultrasound-assisted, and electrochemical precipitation have also been reported.^{32–37} Although these methods are attractive to obtain LDH at a low cost, they are less frequently used because of their complicated experimental procedures.

Hence, we consider that the coprecipitation or urea method is suitable for the industrial production of LDH. Therefore, we developed the improved urea method, in which the CO₂ gas generated by the thermal decomposition of urea is discharged by bubbling a solution with an inert gas. Interestingly, this simple procedure provided us with a technique to directly intercalate selected anions into the LDH without ion exchange. In this study, we describe the preparation of LDH using the urea method and evaluate the crystal structure, morphology, and ionic conductivity of the obtained LDHs.

EXPERIMENTAL SECTION

Preparation of LDH. We prepared Zn–Al LDHs based on the following procedure: Zn(NO₃)₂·6H₂O, Al(NO₃)₃·9H₂O, and urea were dissolved in 100 mL of H₂O ([Al³⁺] = 0.05 mol L⁻¹) with different feed molar ratios of Zn²⁺ and urea to Al³⁺. This aqueous solution was heated in an oil bath under reflux at 120 °C and stirred at 850 rpm for 24 h under an ambient condition or an Ar atmosphere. The resulting white precipitates were filtered under suction (polytetrafluoroethylene (PTFE) membrane, 0.1 mm pore size), washed with distilled water, and then dried for 24 h at 75 °C in air. We also prepared LDHs by changing the divalent metal salts to (i) ZnCl₂ and AlCl₃·6H₂O or (ii) ZnSO₄·7H₂O and Al₂(SO₄)₃. The detailed synthesis conditions are summarized in Table 1.

As a reference, we prepared Zn–Al LDHs using the urea method combined with the hydrothermal process and only the urea method. For the urea method combined with the hydrothermal process, Zn(NO₃)₂·6H₂O, Al(NO₃)₃·9H₂O, and urea were dissolved in 100 mL of H₂O ([Al³⁺] = 0.05 mol L⁻¹) with a feed molar ratio of [Zn²⁺]/[Al³⁺]/[urea] = 2:1:9. Subsequently, the solution was incubated in a stainless steel autoclave at 120 °C for 24 h. The resulting white precipitate was filtered under suction (PTFE membrane, 0.1 mm pore size), washed with distilled water, and then dried for 24 h at 75 °C. The Zn–Al LDH synthesized using only the urea method was prepared by dissolving Zn(NO₃)₂·6H₂O, Al(NO₃)₃·9H₂O and urea in 100 mL of H₂O ([Al³⁺] = 0.05 mol L⁻¹) with a feed molar ratio of [Zn²⁺]/[Al³⁺]/[urea] = 2:1:9 or 2:1:3. The aqueous solution was heated in an oil bath under reflux at 120 °C and stirred at 850 rpm for 24 h in air. The resulting white precipitate was filtered under suction (PTFE membrane, 0.1 mm pore size), washed with distilled water, and then dried for 24 h at 75 °C in air.

Characterization. The interlayer anions of the prepared samples were identified by X-ray diffraction (XRD); the XRD patterns were obtained by a Smart Lab 3K/PD/INP (Rigaku) using CuKα radiation with a scan step of 10° (2θ) for a minute. Each sample was labeled based on the synthesis method, interlayer anions, and a feed molar ratio of Zn and urea to Al, as shown in Table 1. Scanning electron microscopy (SEM, JSM-IT100, JEOL) was used to observe the morphology of the prepared LDHs. The metal cation ratio (Zn²⁺/Al³⁺) of the synthesized LDHs was determined by using inductively coupled plasma emission spectroscopy (ICP, ICPS-8100, Shimadzu).

Impedance Measurement. The ionic conductivities of the prepared LDHs were measured by using the electrochemical impedance method. The LDH powder was pressed at 30 MPa to form pellets with a thickness and diameter of 1.0 and 14 mm, respectively. The Au layers were sputtered on both sides of the pellet for electron conduction, which was then placed in an impedance analyzer (SP-200, BioLogic Science Instruments). The amplitude and frequency range were set to 100 mV and 100 mHz to 7 MHz, respectively. Impedance measurements were performed in a constant-temperature chamber at 80% relative humidity to maintain the temperature and water content.

RESULTS AND DISCUSSION

Characterization of the LDHs. First, we synthesized LDH using a conventional hydrothermal synthesis and urea method. The XRD patterns of H-CO_3^{2-} (2:1:9) are shown by the black line in Figure 1. H-CO_3^{2-} (2:1:9) exhibited several

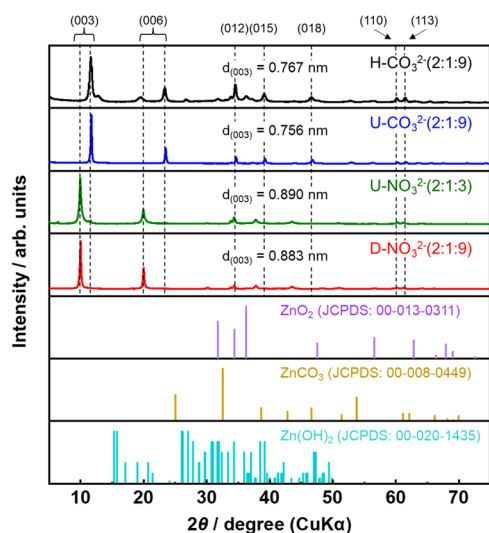


Figure 1. X-ray diffraction (XRD) patterns of layered double hydroxides (LDHs) synthesized by each synthesis method and standard XRD patterns of ZnO_2 (JCPDS No. 00-013-0311), ZnCO_3 (JCPDS No. 00-008-0449), and Zn(OH)_2 (JCPDS No. 00-020-1435). The vertical dotted lines guide the characteristic peaks for the LDHs. The symbol “ $d_{(003)}$ ” in the figure means the vessel space.

characteristic peaks originating from the layered structure of LDH and small peaks originating from byproducts. According to the reference and standard XRD patterns of JCPDS, such side peaks are assigned to mainly ZnO_2 and slightly Zn(OH)_2

and/or ZnCO_3 .³⁸ The byproducts in the hydrothermal synthesis of Zn-Al LDH were already discussed in previous studies.³⁹ In contrast, U-CO_3^{2-} (2:1:9) and U-NO_3^- (2:1:3) exhibited only the characteristic peaks of LDH, which indicate that the high-pressure condition of the hydrothermal process leads to the generation of the byproducts. Note that some weak peaks ascribed to the LDH were not observed due to insufficient signal intensity. The (003) peaks of H-CO_3^{2-} (2:1:9) and U-CO_3^{2-} (2:1:9) were located at 11.6 and 11.7°, respectively, corresponding to basal spacings of 0.767 and 0.756 nm. Conversely, the (003) peak of U-NO_3^- (2:1:3) was located at a lower angle (9.92°), corresponding to a basal spacing of 0.890 nm. This different peak position suggests that NO_3^- was intercalated into the U-NO_3^- instead of CO_3^{2-} considering the fact that the thermodynamic size of NO_3^- is slightly larger than CO_3^{2-} .⁴⁰ Although CO_3^{2-} from urea hydrolysis is typically intercalated instead of NO_3^- in the urea method, our results suggest that the urea method possibly controls the interlayer anions by decreasing the concentration of urea. However, a decrease in the urea concentration is unsuitable because of the deceleration of nucleation and crystal growth. Hence, we considered the bubbling of the solution with an inert gas during the synthesis to decrease the CO_3^{2-} generated from urea while maintaining a sufficient concentration of urea. In this approach, the bubbling with inert gas makes it possible to effectively degas such dissolved gas out. Therefore, we can create a precursor-derived anion-rich environment in the solution, followed by effectively intercalating such a target anion. Based on this, we synthesized LDHs by urea hydrolysis with Ar bubbling. As shown in Figure S1 (Supporting Information), the relative XRD intensity of the (003) peaks corresponding to the LDH layer intercalated with CO_3^{2-} and NO_3^- increased with increasing the feed molar ratio between urea and Al^{3+} under an air atmosphere (without Ar bubbling), whereas a negligibly low intensity of the CO_3^{2-} peak was observed under an Ar atmosphere. Therefore, we

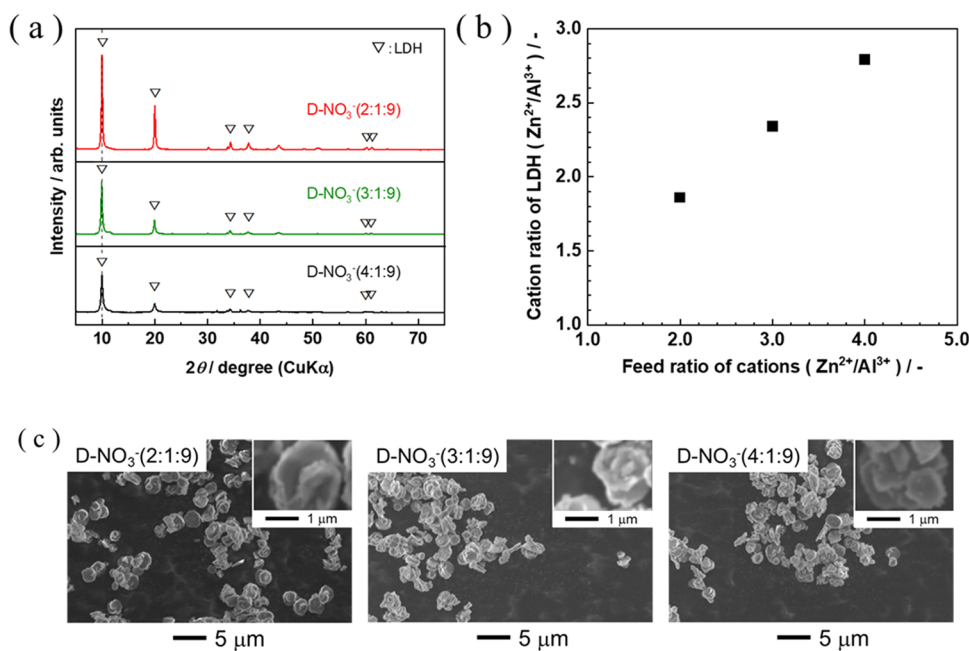


Figure 2. Influence of the feed molar ratio of Zn^{2+} on the synthesis of LDHs using the decarboxylation-urea method. (a) XRD patterns, (b) the metal cation ratio of LDH at different feed ratios of metal ions determined by inductively coupled plasma emission spectroscopy, and (c) scanning electron microscopy (SEM) images.

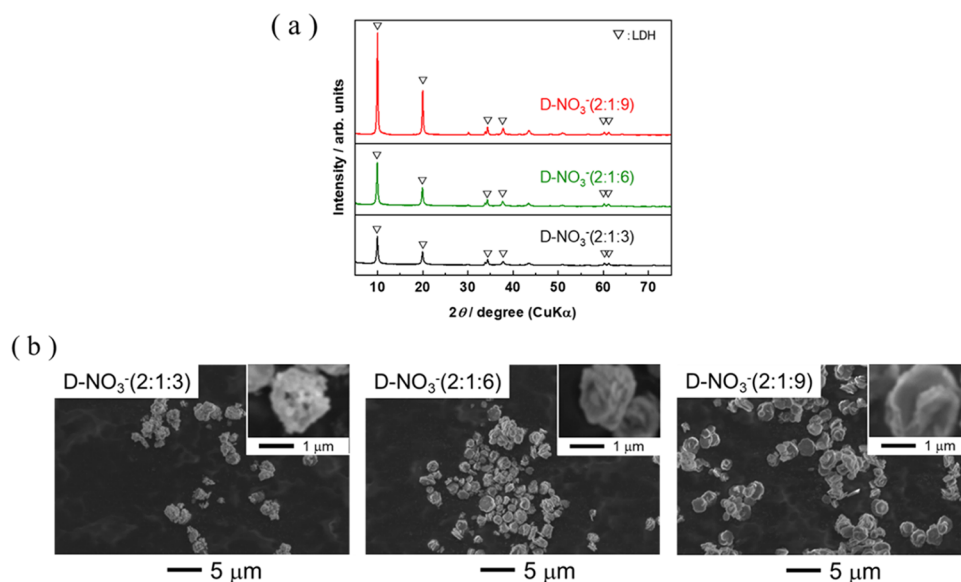


Figure 3. Influence of urea concentration on the synthesis of LDHs using the decarboxylation-urea method, (a) XRD patterns, and (b) SEM images.

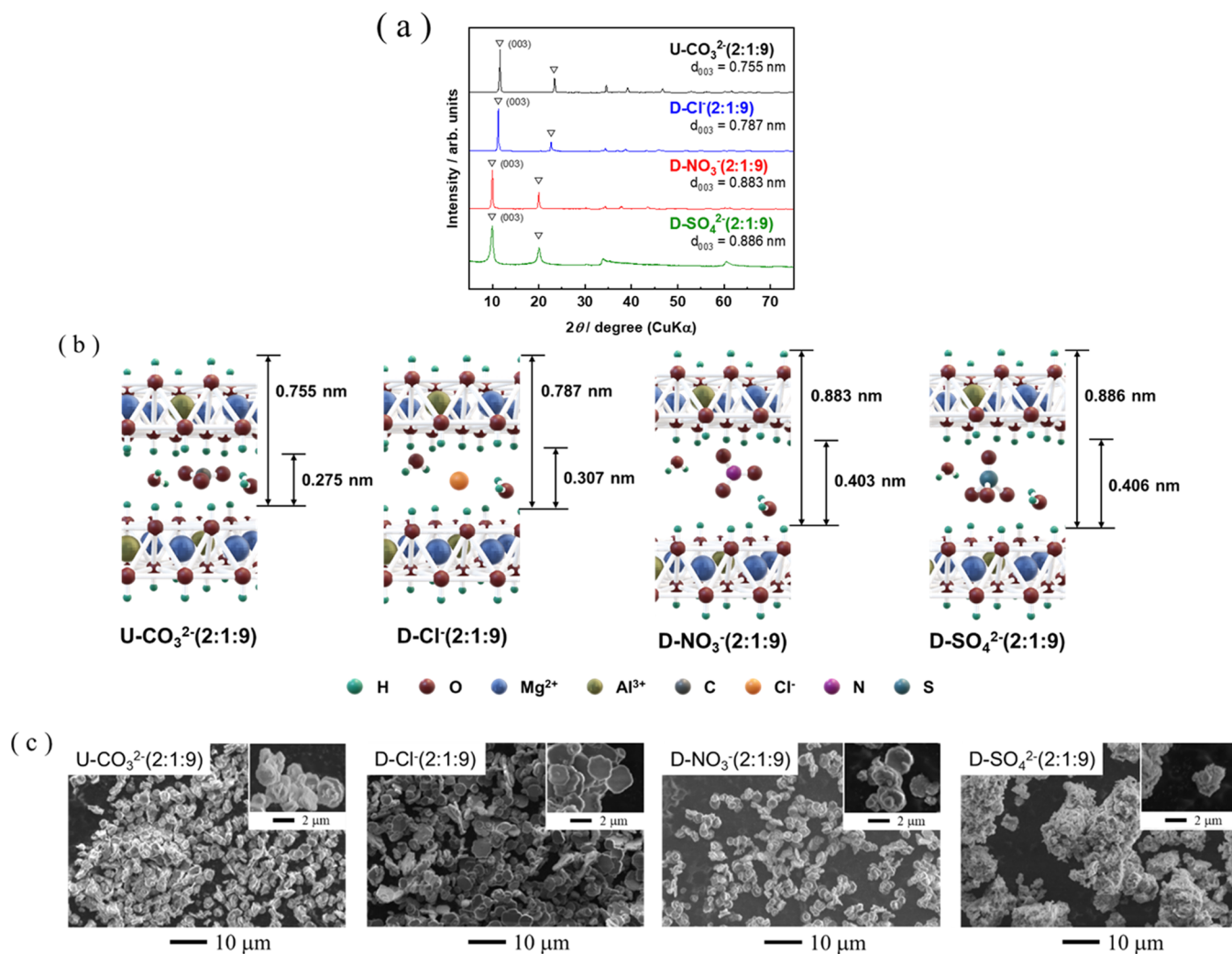


Figure 4. (a) XRD patterns, (b) schematic illustrations of the layered structure expected by XRD, and (c) SEM images of the LDHs synthesized in the presence of different inorganic anions.

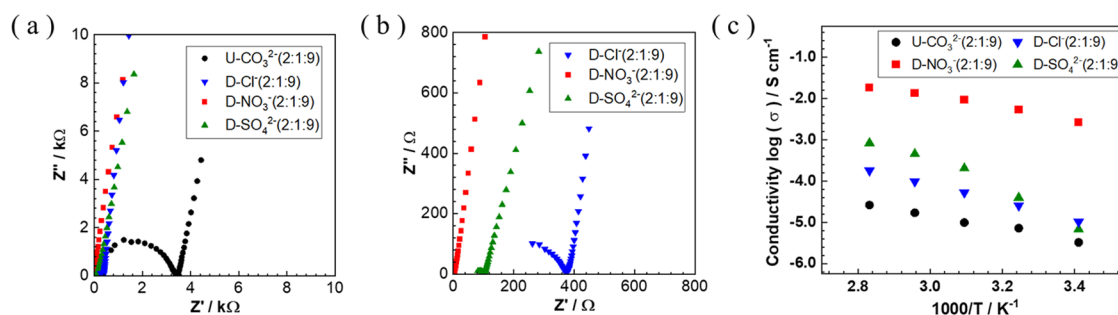


Figure 5. Electrochemical impedance analysis of the prepared LDHs, where panel (a) shows the Nyquist plots, panel (b) is an enlarged figure of (a), and panel (c) illustrates the Arrhenius plots.

obtained LDH intercalated with NO_3^- despite the same concentration of urea as that of $\text{U-CO}_3^{2-}(2:1:9)$ (Figure 1, the lowest panel). This means that the Ar atmosphere is in a better condition to remove CO_3^{2-} , and we labeled this method “decarboxylation-urea method”. The intercalation of other anions into the LDH without ion exchange using this synthesis method is discussed in subsequent sections.

Next, we synthesized LDH with different feed molar ratios of Zn^{2+} . As shown in Figure 2a, the XRD patterns exhibited characteristic peaks of LDH at the same position for all of the synthesized LDHs. In particular, we obtained LDH with similar layered structures despite the fact that the cation ratio ($\text{Zn}^{2+}/\text{Al}^{3+}$) determined by ICP was different (Figure 2b). A similar cation ratio dependence has also been reported for the coprecipitation method.²³ The SEM images showed that the morphology and diameter of the LDH particles were almost identical, with a characteristic plate-like structure of less than 2 μm in all samples (Figure 2c). These results demonstrate that the metal cation ratio barely affected the particle morphology of the LDH.

In contrast, the structure of LDH depended on the urea concentration. Figure 3a shows the XRD patterns of LDHs synthesized with different feed molar ratios of urea. Although the characteristic peaks of LDH were observed in all samples, the particles of $\text{D-NO}_3^-(2:1:3)$ were aggregated, unlike those of $\text{D-NO}_3^-(2:1:6)$ and $\text{D-NO}_3^-(2:1:9)$ (Figure 3b). Furthermore, the size of the LDH particles decreases with a decreasing urea content. This result can be explained by the fact that the crystal growth rate decreases with a decrease in urea. Hence, the concentration of urea plays an important role in the formation of LDH particles in the decarboxylation-urea method, similar to the conventional urea method.

Direct Intercalation of Different Anions. As mentioned above, we demonstrated the possibility that the decarboxylation-urea method intercalates any anions between the layers of LDH instead of CO_3^{2-} , possibly leading to anion-controlled LDH. To focus on this availability, we synthesized LDHs by dissolving inorganic anions (NO_3^- , Cl^- , and SO_4^{2-}) in a precursor solution (Figure 4a). Based on the peak position at (003) in the XRD patterns, we determined the basal spacings to be 0.755 nm (CO_3^{2-}), 0.787 nm (Cl^-), 0.883 nm (NO_3^-), and 0.886 nm (SO_4^{2-}). The difference in the basal spacings suggests that the target anion molecules were intercalated and are in good agreement with previous studies.³⁴⁰ The brucite-like layer of Zn-Al LDH is known to be 0.48 nm,⁴¹ so that we estimated the interlayer distance of each sample to be 0.275 nm (CO_3^{2-}), 0.307 nm (Cl^-), 0.403 nm (NO_3^-), and 0.406 nm (SO_4^{2-}). These structural characteristics of the LDHs are illustrated in Figure 4b. Although the largest interlayer distance

for $\text{D-SO}_4^{2-}(2:1:9)$ had the largest interlayer distance, this can be understood by the fact that SO_4^{2-} is the largest anion in those demonstrated in this study, and the interlayer distances for other samples were different independent of the size of the intercalated anion. Such a dependence of interlayer anion on the interlayer distance might be due to the different structures of interlayer water or hydrated water, which probably result in the different ionic conduction and thermal behaviors of the LDHs.⁴²

Interlayer anions usually follow ion-exchange equilibrium constants in the order of $\text{CO}_3^{2-} > \text{SO}_4^{2-} > \text{OH}^- > \text{F}^- > \text{Cl}^- > \text{Br}^- > \text{NO}_3^- > \text{I}^-$. In contrast, our observations strongly indicate that the selected anion is intercalated regardless of the ion-exchange equilibrium constants. This indicates that CO_3^{2-} was effectively removed from the system during the reaction without intercalation into the LDH. The intercalated anion species were also confirmed by FT-IR measurements (Supporting Information, Figure S2). Therefore, the decarboxylation-urea method is suitable for the synthesis of anion-controlled LDHs.

From the SEM observations, we found another aspect of the morphology and structure of LDH (Figure 4c). Except for the SO_4^{2-} type, plate-like particles were clearly observed, in which the diameters of these particles were 2 mm for $\text{D-Cl}^-(2:1:9)$ and less than 2 mm for $\text{U-CO}_3^{2-}(2:1:9)$ and $\text{D-NO}_3^-(2:1:9)$. This difference suggests that the anions in the precursor solution have a possible effect on the crystal growth. Another possibility is that the basal spacing of the LDH might affect the size of the LDH particles. However, the size of the particles barely affected the basal spacing because the basal spacings of $\text{U-CO}_3^{2-}(2:1:9)$ and $\text{D-NO}_3^-(2:1:9)$ differed greatly despite their similar particle sizes. The $\text{D-SO}_4^{2-}(2:1:9)$ particles aggregated with each other, which could be due to the generation of byproducts, such as alunit, from sulfate and aluminum ions (Figure S3). Therefore, the LDH prepared by the decarboxylation-urea method controlled the morphology and size of the LDH particles via anions in the precursor solution.

Ionic Conductivity. Finally, we conducted ionic conductivity measurements of the prepared LDHs using the electrochemical impedance method to evaluate their performance in electrochemical devices, such as electrolytes. Figure 5a,b shows the complex impedance plots (100 mHz to 7 MHz) for LDHs with different interlayer anion species at 80 °C and 80% relative humidity. In each Nyquist plot, we observed two relaxation modes: a semicircle at the high-frequency region and a straight-like curve at the low-frequency region. The faster relaxation corresponds to a grain boundary resistance (or mass transfer resistance), and the slower relaxation is related to an

interface resistance between LDH and electrode. On the other hand, a relaxation mode ascribed to a bulk resistance (or charge-transfer resistance) was hardly observed because of insufficient frequency range or was an indistinguishable contribution from a grain boundary resistance. Here, we determined ionic conductivity based on the following equation

$$\sigma = \frac{L}{R \times A}$$

where σ (S cm⁻¹), L (cm), R (W), and A (cm²) are the ionic conductivity, thickness, resistance, and measurement area of the pellet, respectively. The resistance value was obtained from the cross section of the semicircle and X-axis, which is the total resistance of the bulk and grain boundary resistances. Figure 5c illustrates the temperature dependence of the ionic conductivity (Arrhenius plots) of the prepared LDHs. The ionic conductivities of all of the samples increased with temperature and differed in each sample. The ionic conductivity at 80 °C decreased in the order of D-NO₃⁻(2:1:9) > D-SO₄²⁻(2:1:9) > D-Cl⁻(2:1:9) > U-CO₃²⁻(2:1:9). In particular, the LDH intercalated with NO₃⁻ exhibited the highest ionic conductivity (D-NO₃⁻(2:1:9):18.0 mS cm⁻¹), which is also higher than that reported in other studies using the coprecipitation method and hence suitable for electrochemical applications.^{16,17} Zhang et al. reported that smaller-sized LDHs had higher ionic conductivity due to much adsorbed water on the surface of LDH particles.⁴³ However, although the particle sizes of U-CO₃²⁻(2:1:9) and D-NO₃⁻(2:1:9) were similar, the ionic conductivity of D-NO₃⁻(2:1:9) was more than 10³ times higher than that of U-CO₃²⁻(2:1:9). Therefore, the ionic conductivity should be dominated by the mobility of the interlayer anions in the LDH particles. What is the important point here is that the slope of the plots in each sample gave us similar activation energy for ionic conduction (ca. 20 kJ/mol) except for D-SO₄²⁻(2:1:9). The larger activation energy for D-SO₄²⁻(2:1:9) might be due to the presence of the byproduct described in Figure 4b. These indicate that OH⁻ ions liberated from interlayer water are the dominant species for ionic conduction regardless of the interlayer anion species. However, our impedance data does not clearly provide information on the bulk resistance, and thus, it is difficult to separately discuss the anion mobility inside the basal space of the LDH. Nevertheless, the difference in the conditions of interlayer water by the interlayer anion species may be a possibility. In future work, we will investigate the diffusibility and bonding of the interlayer water.

CONCLUSIONS

We developed a one-pot synthesis method for LDHs intercalated with selected anions. The crystalline structures, particle morphologies, and ionic conductivities of the obtained LDHs were assessed. In the conventional urea method, controlling the interlayer anions is difficult in one-pot systems because the LDH intercalates with CO₃²⁻ that is generated by the hydrolysis of urea. In contrast, we synthesized LDH intercalated with selected anions by Ar bubbling to remove CO₃²⁻ in a one-pot process. This method was labeled as the “decarboxylation-urea method”. Consequently, the LDHs synthesized using our method were endowed with the following characteristics: (1) the metal cation ratio of the prepared LDHs reflects the metal cation concentration of the precursor solution. (2) The morphology of the prepared LDH particles was affected by the concentration of urea in the

precursor solution, and the particle size increased with the increasing concentration of urea. (3) The morphology of the prepared LDH particles depends on the anion species in the precursor solution. (4) The ionic conductivity of LDH varied with the interlayer anions, and the Zn–Al LDH intercalated with NO₃⁻ showed the highest ionic conductivity of 18 mS cm⁻¹. These results indicate that the decarboxylation-urea method has a high versatility for LDH synthesis. We believe that this study will provide a novel technique to afford interlayer-anion-controlled LDHs and provide new insights into the effects of interlayer anions on the physical properties and morphologies of LDHs.

ASSOCIATED CONTENT

Supporting Information

The Supporting Information is available free of charge at <https://pubs.acs.org/doi/10.1021/acsomega.3c04650>.

LDH preparation and their XRD analysis for comparing the conventional urea method with the decarboxylation-urea method (Figure S1), the FT-IR measurement of the prepared LDH for confirmation of the intercalated anion species using the decarboxylation-urea method (Figure S2), and the X-ray diffraction pattern and scanning electron microscopy image of the sample synthesized under high concentration of sulfate ions (Figure S3) (PDF)

AUTHOR INFORMATION

Corresponding Author

Hirohisa Yamada – Department of Chemical Engineering, National Institute of Technology, Nara College, Nara 639-1080, Japan; orcid.org/0000-0003-0958-1529; Phone: +81-743-55-6157; Email: yamada@nara.kosen.ac.jp

Authors

Masahiro Uga – Department of Chemical Engineering, National Institute of Technology, Nara College, Nara 639-1080, Japan

Yusuke Taniguchi – Department of Chemical Engineering, National Institute of Technology, Nara College, Nara 639-1080, Japan

Mitsuhiro Matsumoto – Department of Chemical Engineering, National Institute of Technology, Nara College, Nara 639-1080, Japan; orcid.org/0000-0003-0748-8355

Takuya Okada – Department of Chemical Engineering, National Institute of Technology, Nara College, Nara 639-1080, Japan

Kazuki Maeda – Kyoisha Chemical Co., Ltd., Nara 630-8453, Japan

Eiko Mieda – Graduate School of Science Molecular Materials Science Course, Osaka Metropolitan University, Osaka 558-8585, Japan

Katsumi Katakura – Department of Chemical Engineering, National Institute of Technology, Nara College, Nara 639-1080, Japan

Complete contact information is available at:

<https://pubs.acs.org/doi/10.1021/acsomega.3c04650>

Author Contributions

M.U. synthesized and characterized layered double hydroxides and measured the ionic conductivities of prepared layered

double hydroxides and wrote the first draft of the paper. Y.T. synthesized and characterized layered double hydroxides. M.M. discussed the results, commented on the manuscript, and revised the paper. T.O., K.M., E.M., and K.K. discussed the results. H.Y. conceived and supervised the study. All authors have given approval to the final version of the manuscript.

Notes

The authors declare no competing financial interest.

ACKNOWLEDGMENTS

This work was supported by JSPS KAKENHI Grant Nos. 19K05682 and 21H00811. Part of this study was supported by a project, Gear of Education and Advanced Resources (Gear5.0), organized by the National Institute of Technology (KOSEN). The authors would like to thank Editage (www.editage.com) for English language editing.

ABBREVIATIONS

ICP, inductively coupled plasma emission spectroscopy; LDH, layered double hydroxide; PTFE, polytetrafluoroethylene; SEM, scanning electron microscopy; XRD, X-ray diffraction

REFERENCES

- (1) Fogg, A. M.; Freij, A. J.; Parkinson, G. M. Synthesis and anion exchange chemistry of rhombohedral Li/Al layered double hydroxides. *Chem. Mater.* **2002**, *14*, 232–234.
- (2) Miyata, S. Anion-exchange properties of hydrotalcite-like compounds. *Clays Clay Miner.* **1983**, *31*, 305–311.
- (3) Iyi, N.; Fujii, K.; Okamoto, K.; Sasaki, T. Factors influencing the hydration of layered double hydroxides (LDHs) and the appearance of an intermediate second staging phase. *Appl. Clay Sci.* **2007**, *35*, 218–227.
- (4) Miyata, S. The syntheses of hydrotalcite-like compounds and their structures and physico-chemical properties-i: The systems Mg²⁺-Al³⁺-NO₃⁻, Mg²⁺-Al³⁺-Cl⁻, Mg²⁺-Al³⁺-ClO₄⁻, Ni²⁺-Al³⁺-Cl⁻ and Zn²⁺-Al³⁺-Cl⁻. *Clays Clay Miner.* **1975**, *23*, 369–375.
- (5) Miyata, S. Physico-Chemical Properties of Synthetic Hydrotalcites in Relation to Composition. *Clays Clay Miner.* **1980**, *28*, 50–56.
- (6) Zhao, Y.; He, S.; Wei, M.; Evans, D. G.; Duan, X. Hierarchical films of layered double hydroxides by using a sol-gel process and their high adaptability in water treatment. *Chem. Commun.* **2010**, *46*, 3031–3033.
- (7) Li, L.; Gu, W.; Chen, J.; Chen, W.; Xu, Z. P. Co-delivery of siRNAs and anti-cancer drugs using layered double hydroxide nanoparticles. *Biomaterials* **2014**, *35*, 3331–3339.
- (8) Liang, H.; Lin, J.; Jia, H.; et al. Hierarchical NiCo-LDH@NiOOH core-shell heterostructure on carbon fiber cloth as battery-like electrode for supercapacitor. *J. Power Sources* **2018**, *378*, 248–254.
- (9) Iyi, N.; Matsumoto, T.; Kaneko, Y.; Kitamura, K. Deintercalation of carbonate ions from a hydrotalcite-like compound: Enhanced decarbonation using acid-salt mixed solution. *Chem. Mater.* **2004**, *16*, 2926–2932.
- (10) Li, B.; He, J.; Evans, D. G.; Duan, X. Inorganic layered double hydroxides as a drug delivery system - Intercalation and in vitro release of fenbufen. *Appl. Clay Sci.* **2004**, *27*, 199–207.
- (11) Wu, X. L.; Wang, L.; Chen, C. L.; Xu, A. W.; Wang, X. K. Water-dispersible magnetite-graphene-LDH composites for efficient arsenate removal. *J. Mater. Chem.* **2011**, *21*, 17353–17359.
- (12) Yin, Q.; Rao, D.; Zhang, G.; et al. CoFe-Cl Layered Double Hydroxide: A New Cathode Material for High-Performance Chloride Ion Batteries. *Adv. Funct. Mater.* **2019**, *29*, No. 1900983.
- (13) de Roy, A.; Besse, J. P. Evolution of protonic conduction in some synthetic anionic clays. *Solid State Ionics* **1991**, *46*, 95–101.
- (14) Ducos, V.; De Roy, A.; Besse, J. P. Evolution of protonic conduction in [Zn-Al-Cl] Lamellar double hydroxide phases with temperature and trivalent metal content. *Solid State Ionics* **2001**, *145*, 399–405.
- (15) Kubo, D.; Tadanaga, K.; Hayashi, A.; Tatsumisago, M. Improvement of electrochemical performance in alkaline fuel cell by hydroxide ion conducting NiAl layered double hydroxide. *J. Power Sources* **2013**, *222*, 493–497.
- (16) Sun, P.; Ma, R.; Bai, X.; et al. Single-layer nanosheets with exceptionally high and anisotropic hydroxyl ion conductivity. *Sci. Adv.* **2017**, *3*, No. e1602629, DOI: 10.1126/sciadv.1602629.
- (17) Furukawa, Y.; Tadanaga, K.; Hayashi, A.; Tatsumisago, M. Evaluation of ionic conductivity for Mg-Al layered double hydroxide intercalated with inorganic anions. *Solid State Ionics* **2011**, *192*, 185–187.
- (18) Hu, J.; Tang, X.; Dai, Q.; et al. Layered double hydroxide membrane with high hydroxide conductivity and ion selectivity for energy storage device. *Nat. Commun.* **2021**, *12*, No. 3409.
- (19) Miyazaki, K.; Asada, Y.; Fukutsuka, T.; Abe, T.; Bendersky, L. A. Structural insights into ion conduction of layered double hydroxides with various proportions of trivalent cations. *J. Mater. Chem. A* **2013**, *1*, 14569–14576.
- (20) Dupin, J. C.; Martinez, H.; Guimon, C.; Dumitriu, E.; Fechete, I. Intercalation compounds of Mg-Al layered double hydroxides with dichlophenac: Different methods of preparation and physico-chemical characterization. *Appl. Clay Sci.* **2004**, *27*, 95–106.
- (21) Marchi, A. J.; Apesteguía, C. R. Impregnation-induced memory effect of thermally activated layered double hydroxides. *Appl. Clay Sci.* **1998**, *13*, 35–48.
- (22) Panda, H. S.; Srivastava, R.; Bahadur, D. Synthesis and in situ mechanism of nuclei growth of layered double hydroxides. *Bull. Mater. Sci.* **2011**, *34*, 1599–1604.
- (23) Zhao, Y.; Li, F.; Zhang, R.; Evans, D. G.; Duan, X. Preparation of layered double-hydroxide nanomaterials with a uniform crystallite size using a new method involving separate nucleation and aging steps. *Chem. Mater.* **2002**, *14*, 4286–4291.
- (24) Xu, Z. P.; Stevenson, G.; Lu, C. Q.; Lu, G. Q. Dispersion and size control of layered double hydroxide nanoparticles in aqueous solutions. *J. Phys. Chem. B* **2006**, *110*, 16923–16929.
- (25) Ogawa, M.; Kaiho, H. Homogeneous precipitation of uniform hydrotalcite particles. *Langmuir* **2002**, *18*, 4240–4242.
- (26) Costantino, U.; Marmottini, F.; Nocchetti, M.; Viviani, R. New synthetic routes to hydrotalcite-like compounds - Characterisation and properties of the obtained materials. *Eur. J. Inorg. Chem.* **1998**, *1998*, 1439–1446.
- (27) Vial, S.; Prevot, V.; Forano, C. Novel route for layered double hydroxides preparation by enzymatic decomposition of urea. *J. Phys. Chem. Solids* **2006**, *67*, 1048–1053.
- (28) Wei, Y.; Li, F.; Liu, L. Liquid exfoliation of Zn-Al layered double hydroxide using NaOH/urea aqueous solution at low temperature. *RSC Adv.* **2014**, *4*, 18044–18051.
- (29) Wu, X.; Du, Y.; An, X.; Xie, X. Fabrication of NiFe layered double hydroxides using urea hydrolysis - Control of interlayer anion and investigation on their catalytic performance. *Catal. Commun.* **2014**, *50*, 44–48.
- (30) Szabados, M.; Kónya, Z.; Kukovecz, Á.; Sipos, P.; Pálkó, I. Structural reconstruction of mechanochemically disordered CaFe-layered double hydroxide. *Appl. Clay Sci.* **2019**, *174*, 138–145.
- (31) Nakayama, H.; Wada, N.; Tshako, M. Intercalation of amino acids and peptides into Mg-Al layered double hydroxide by reconstruction method. *Int. J. Pharm.* **2004**, *269*, 469–478.
- (32) Yang, Z.; Choi, K. M.; Jiang, N.; Park, S. E. Microwave synthesis of hydrotalcite by urea hydrolysis. *Bull. Korean Chem. Soc.* **2007**, *28*, 2029–2033.
- (33) Chubar, N.; Gerda, V.; Megantari, O.; et al. Applications versus properties of Mg-Al layered double hydroxides provided by their syntheses methods: Alkoxide and alkoxide-free sol-gel syntheses and hydrothermal precipitation. *Chem. Eng. J.* **2013**, *234*, 284–299.

(34) Jia, Q.; Gao, J.; Qiu, C.; et al. Ultrasound-seeded vapor-phase-transport growth of boundary-rich layered double hydroxide nano-sheet arrays for highly efficient water splitting. *Chem. Eng. J.* **2022**, *433*, No. 134552.

(35) Ay, A. N.; Zümreoglu-Karan, B.; Mafra, L. A simple mechanochemical route to layered double hydroxides: synthesis of hydrotalcite-like Mg-Al-NO₃-LDH by Manual Grinding in a Mortar. *Z. Anorg. Allg. Chem.* **2009**, *635*, 1470–1475.

(36) Crepaldi, E. L.; Pavan, P. C.; Valim, J. B. A new method of intercalation by anion exchange in layered double hydroxides. *Chem. Commun.* **1999**, 155–156.

(37) Dixit, M.; Vishnu Kamath, P. Electrosynthesis and stabilization of α -cobalt hydroxide in the presence of trivalent cations. *J. Power Sources* **1995**, *56*, 97–100.

(38) Winiarski, J.; Tylus, W.; Winiarska, K.; Szczygiel, I.; Szczygiel, B. XPS and FT-IR Characterization of Selected Synthetic Corrosion Products of Zinc Expected in Neutral Environment Containing Chloride Ions. *J. Spectrosc.* **2018**, *2018*, 1–14, DOI: 10.1155/2018/2079278.

(39) Thevenot, F.; Szymanski, R.; Chaumette, P. Preparation and characterization of Al-rich Zn-Al hydrotalcite-like compound. *Clays Clay Miner.* **1989**, *16*, 396–402.

(40) Roobottom, H. K.; Jenkins, H. D. B.; Passmore, J.; Glasser, L. Thermochemical Radii of Complex Ions. *J. Chem. Educ.* **1999**, *76*, 1570–1572.

(41) Prestopino, G.; Arrabito, G.; Generosi, A.; et al. Emerging switchable ultraviolet photoluminescence in dehydrated Zn/Al layered double hydroxide nanoplatelets. *Sci. Rep.* **2019**, *9*, No. 11498.

(42) Aisawa, S.; Hirahara, H.; Uchiyama, H.; Takahashi, S.; Narita, E. Synthesis and thermal decomposition of Mn-Al layered double hydroxides. *J. Solid State Chem.* **2002**, *167*, 152–159.

(43) Zhang, P.; Yamaguchi, T.; Nair, B.; Miyajima, K.; Anilkumar, G. M. Mg-Al Layered double hydroxides: A correlation between synthesis-structure and ionic conductivity. *RSC Adv.* **2014**, *4*, 41051–41058.